Supplementary Information on geochronology

Age models were based on downcore radionuclide activities (^{241}Am, ^{210}Pb), as well as on six calibrated radiocarbon ages for both the Callao and the Pisco cores. For Callao, the model was constrained by relating stratigraphic anomalies with information of large historic marine earthquakes that had rupture zones near the core site (Dorbath et al., 1990).

In order to avoid compaction artefacts, sedimentation models were calculated using mass accumulation rather than sediment depth. Age-mass models were developed removing stratigraphic anomalies believed to be instantaneous deposits, as the Pisco core presented one slump near the bottom and the Callao core presented two nearly contiguous slumps in the mid-section and another one near the bottom.

Protruding filaments of the giant sulphur bacteria *Thioploca* spp., which lives in the sediment water interface, were observed in the core tops and hence, confirmed that the sediment surface was recovered in both box cores. In the uppermost layer, the downcore profiles of the bomb-derived ^{241}Am was used to date both cores as bomb-derived radionuclides reflect fallout due to atomic bomb testing in both hemispheres since 1953 (Appleby, 2000; UNSCEAR, 2000; Ribeiro & Arribére, 2002). Below the appearance of ^{241}Am in the sediments, excess ^{210}Pb activities were used to fit sedimentation models until values reached the ^{210}Pb time-domain, which is considered to be equivalent to six half-lives of ^{210}Pb before present, approximately 135 years ago (Figure S1). While the downcore distribution of excess ^{210}Pb closely followed an exponential curve in the Callao core, the downcore distribution in the Pisco core exhibited some scattering. Therefore a constant flux, constant supply CFCS sedimentation model was applied to the Callao core whereas a constant rate supply CRS sedimentation model (that assumes varying sedimentation rate) was applied for to the Pisco core (Appleby, 2000).

Radiocarbon ages of bulk organic matter were used to date the lower section of the cores. The radiocarbon ages increased with accumulated mass but with some scatter, particularly in the case of the Pisco core. Old radiocarbon ages leading to age inversions due to anomalously higher local reservoir age or changing organic matter source were not used in the age model construction. For elucidating the origin of organic matter, sediment samples were examined under the petrographic microscope (transmitted light), after separation from carbonate-bearing and silicate phases using acid digestion (palynofacies analysis). This approach leads to the identification of the different organic components and provides a quantitative estimation of their relative abundance (Boussafir et al., 1995).

The downcore profiles of the organic fraction (Palynofacies), Oxygen Index (Rock-Eval) and total organic carbon against conventional radiocarbon ages and $\delta^{13}C$ of the dated samples revealed the existence of two groups, according to the organic matter characteristics (Figure S2). The first group, which is dominant, was associated with high content of homogenous amorphous marine organic matter, a signature that is associated with high productivity linked to upwelling (Boussafir et al., 1995; Pichevin et al., 2004), and relatively low Oxygen Index values. The group was found mostly throughout the Callao core, and mainly above the lithological shift in the Pisco core. Only one inversion towards older radiocarbon age was identified in this group associated with the shift in the Callao core (Figure S2a), which was interpreted as an amplification of the local reservoir age, due to water mass change or stronger upwelling. Hence, with the exception of this point, this group was used for the age model development.

The second group or organic carbon appeared below the lithological shift, particularly in the Pisco core. It was characterized by anomalously old radiocarbon ages leading to significant age inversions, increased content of dispersed amorphous organic matter (AOM) or increased content of terrestrial plants matter, relatively high values of Oxygen Index, and very negative values of $\delta^{13}C$ (< -22.5 ‰). Taken together these signatures indicate the contribution of allochtonous, reworked, or even terrestrial

organic matter (Meyers et al., 1997), explaining the older than expected radiocarbon ages (Figure S2b). Therefore, radiocarbon values from this group were not taken into account for the age model development.

The radiocarbon age associated to the shift in the Pisco core was better aligned with the radiocarbon ages in the upper part of the core, so we applied the average local reservoir age (DR) during the ^{210}Pb-time domain (292 ± 50 y), computed by difference with the ^{210}Pb-derived dates, to calibrate this data point. The average DR within the ^{210}Pb-time domain was estimated by applying a linear regression fit to the downcore radiocarbon ages versus the accumulated mass up to the oldest ^{210}Pb-dating point, which had an accumulated mass set to zero. The marine calibration curve (Hughen et al., 2004) was used to determine the average marine reservoir age for the period. The average local reservoir age (DR) was taken as the difference between the regression curve intercept and the average marine reservoir age plus the ^{210}Pb-derived age (Figure S3). In turn, these DR ages were used to determine the calibrated radiocarbon ages, using the software CALIB v. 5.0 (Stuiver & Reimer, 1993; Stuiver et al., 2005). After the calibration, the average mass accumulation rate (MAR) before the ^{210}Pb time-domain was obtained by linear regression of the calibrated radiocarbon ages versus the accumulated mass, including the oldest ^{210}Pb-dating point.

For the Callao core, the average MAR is 0.0174 ± 0.0012 g cm^{-2} y^{-1} (n=7, R^2= 0.98), yielding an age of the record of about 720 years. If only the core section between the second and third slump is used, the computed MAR is similar (0.0177 ± 0.0032 g cm^{-2} y^{-1}; n=4, R^2=0.92), and the intercept at the second slump position is 1660 ± 43 AD. Applying either of the two rates, the two contiguous slumps are dated about 47 years apart. The two largest historic marine earthquakes that hit Callao occurred within 59 years, at 1746 AD (8.6 Mw) and at 1687 AD (8.0 Mw) (Dorbath et al., 1990). Thus the two slumps very likely correspond to the two seismic events, with some sediment loss, and we used the earthquake dates as time-markers for the age model.

The average MAR before the ^{210}Pb-time domain mentioned above is significantly lower than the ^{210}Pb-CFCS MAR (0.0306 ± 0.0030 g cm^{-2} y^{-1}, n=6). Thin-section observations across the lithological shift, indicate it represents a real stratigraphic boundary between sedimentation regimes. Applying the average MAR computed before and the 1746-slump time marker the shift was dated at 1818 ± 6 AD. In turn, the MAR for the time period between 1860 AD and the shift date could be estimated as 0.0207 ± 0.0046 g cm^{-2} y^{-1} (Figure 2a).

For the Pisco core, the average MAR is 0.0218 ± 0.0013 g cm^{-2} y^{-1} (n=7, R^2= 0.92), yielding an age of the record of about 705 years. The rate was significantly lower than the mean ^{210}Pb-CRS MAR, computed for the period between ca. 1935 AD and 1860 AD, when variation in velocity of sediment accumulation was little (0.0297 ± 0.0067 g cm^{-2} y^{-1}, n = 14). Using the average MAR, the lithological shift is dated at 1812 ± 7 AD, which is younger than the date based on the ^{210}Pb-CRS model, though within statistical range (1825 ± 9 AD). Following the same approach as for the Callao core, here it is concluded that the lithological shift is a real stratigraphic boundary. Since dating resolution here is not sufficient to directly resolve changes in sedimentation across the lithological shift, we estimated the shift date as the mean value from the two estimated dates (1819 ± 12 AD). The sedimentation rate for the time period between 1860 AD and the shift date was then estimated (0.0251 ± 0.0063 g cm^{-2} y^{-1}) as done in the Callao core (Figure 2b).

In summary, the final age model for both cores included: 1) the ^{241}Am/^{210}Pb-derived MAR models from the oldest ^{210}Pb derived-dated point to the present; 2) the intermediate MAR between the shift date and the oldest ^{210}Pb derived-dated point; and 3) the average MAR, based on calibrated ^{14}C ages, for the whole period until the sedimentological shift.

Supplementary references

1. Appleby, P.G. Chronostratigraphic techniques in recent sediments. In: *Developments in Paleoenvironmental Research. Volume 1, Tracking Environmental Changes in Lake Sediments: Physical and Chemical Techniques* (eds. Last W.M. & Smol J.P), 171- 203 (Kluwer, Dordrecht, The Netherlands, 2000)

2. Boussafir, M., Gelin, F., Lallier-Vergès, E., Derenne, S., Bertrand, P., Largeau, C. Electron microscopy and pyrolysis of kerogens from Kimmeridge Clay Formation, UK: source organisms, preservation processes and origin of microcycles. 1995. *Geochim. Cosmochim. Acta*, 59: 3731–3747 (1995)

3. Dorbath, L., Cisternas, A. and Dorbath, C. Assessment of the size of large and great historical earthquakes in Peru. *Bull. Seismol. Soc. Amer*., 80, 551-576 (1990)

4. Hughen, K. A. et al. Marine04 Marine Radiocarbon Age Calibration, 0-26 Cal Kyr BP. *Radiocarbon*, 46, 1059-1086 (2004)

5. Meyers, P.A. Organic geochemical proxies of paleoceanographic, paleolimnologic, and paleoclimatic processes. *Org. Geochem*., 27, 213–250 (1997)

6. Pichevin, L., Bertrand, P., Boussafir, M., Disnar, J.-R. Organic matter accumulation and preservation controls in a deep sea modern environment: an example from Namibia slope sediments. *Org. Geochem*., 35, 543–559 (2004)

7. Ribeiro Guevara, S. and Arribére, M. ^{137}Cs dating of lake cores from the Nahuel Huapi National Park, Patagonia, Argentina: Historical records and profile measurements. *J. Rad. Nucl. Chem*., 252, 37–45 (2002)

8. Stuiver, M., and Reimer, P. J. Extended ^{14}C database and revised CALIB radiocarbon calibration program, *Radiocarbon*, 35, 215-230 (1993)

9. Stuiver, M., Reimer, P. J., and Reimer, R. W. CALIB 5.0. [WWW program and documentation]. http://calib.qub.ac.uk/calib/ (2005)

10. United Nations Scientific Committee on the Effects of Atomic Radiation UNSCEAR. *Report to the General Assembly, with scientific anexes. Annex C. Exposures to the public from man-made radiations*. 134 p. (Vienna, 2000)

Supplementary Figure 1

Downcore profiles of excess ^{210}Pb and ^{241}Am in the Callao boxcore B0413 (a) and in the Pisco boxcore B0406 (b). c) reconstructed fallout of ^{137}Cs in the Southern Hemisphere (UNSCEAR, 2000), and fallout specific activity of ^{137}Cs in Buenos Aires (Ribeiro & Arribére, 2002). The prominent features of fallout change (onset and peak periods, shaded) were used to identify three time-markers in the downcore ^{241}Am specific activity for both cores. Time intervals for each time-marker were estimated from excess ^{210}Pb – derived sedimentation rate in the uppermost layer and sample layer thickness.

Supplementary Figure 2

X-ray digital radiographies and downcore profiles of total organic carbon content (%), Rock Eval Oxygen Index (mg O g TOC^{-1}), palynofacies analysis of the organic matter, conventional radiocarbon ages and δ^{13}C of the radiocarbon samples in the Callao boxcore (a) and in the Pisco boxcore (b). The dotted lines highlight old radiocarbon ages leading to significant age inversions (yellow circles) in relation with organic matter properties (see supplementary text on methods). Radiocarbon ages in white circles correspond to the ^{210}Pb-time domain and were not used in the model. Amplifications of the three slumps in the Callao core and of the slump in the Pico core are showed at left and dotted. The gaps in the Y-axes of the downcore profiles indicate the slumps' positions.

Supplementary Figure 3

Estimation of the local reservoir age (DR) before the late nineteenth century (core B0406, Pisco). A linear regression between conventional ^{14}C age and accumulated mass

before the ^{210}Pb time domain, yields the approximate age BP of the record, for which the average ocean reservoir age (R) is calculated, using the marine calibration curve (Hughen et al., 2004). The difference between the curve intercept and the age BP of the origin (90 ± 5 BP, according to the ^{210}Pb CRS model) is the total reservoir effect (DR + R). Thus DR is the difference between the total reservoir effect and the average ocean reservoir age (188 ± 79 years). The same procedure applied for the Callao box core yielded a DR value equal to 279 ± 53 years.

SF1

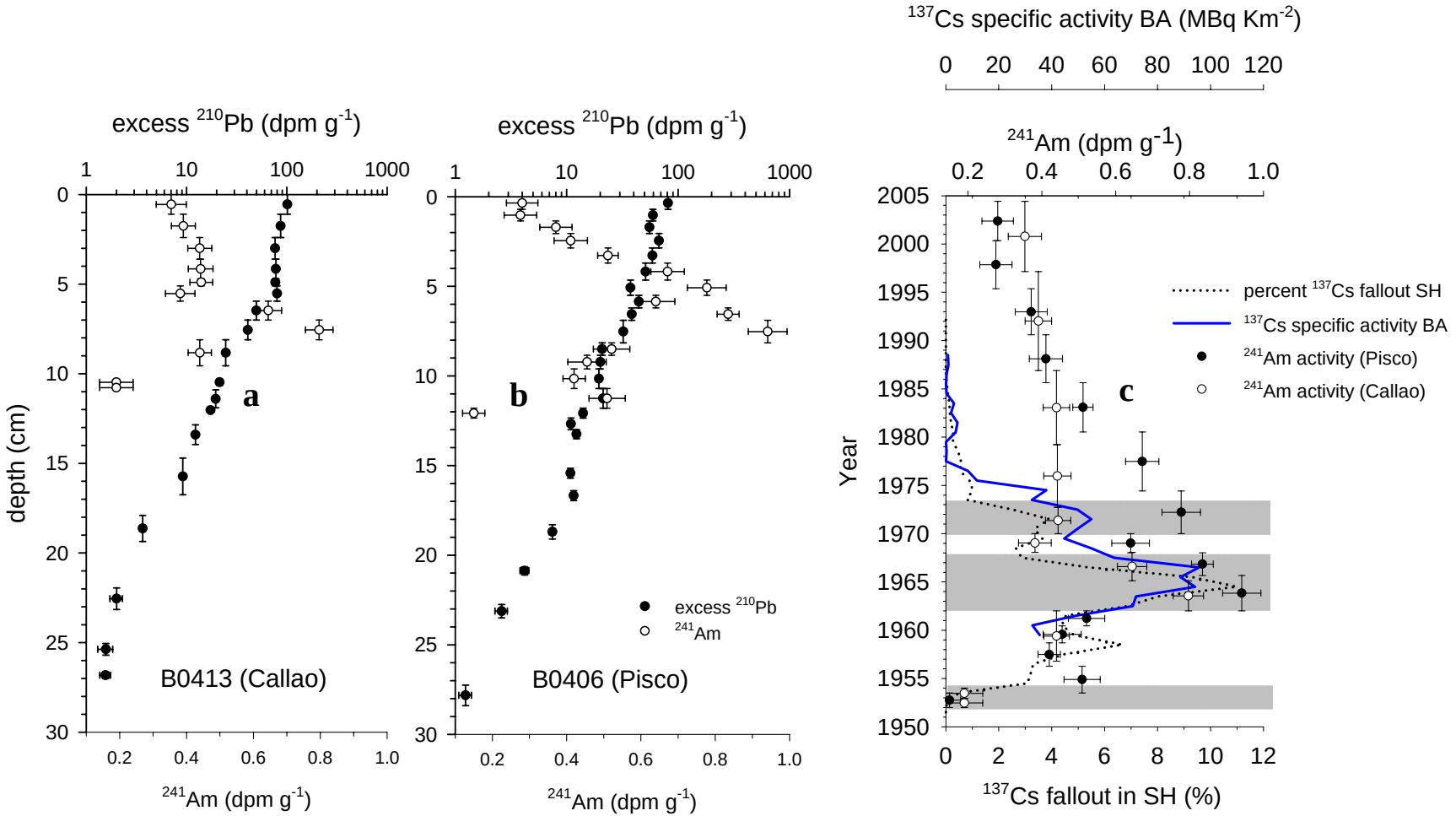
excess 210Pb (dpm g-1)
depth (cm)
a
B0413 (Callao)
241Am (dpm g-1)
b
B0406 (Pisco)
excess 210Pb
241Am
137Cs specific activity BA (MBq Km-2)
241Am (dpm g-1)
Year
c
percent 137Cs fallout SH
137Cs specific activity BA
241Am activity (Pisco)
241Am activity (Callao)
137Cs fallout in SH (%)

SF2

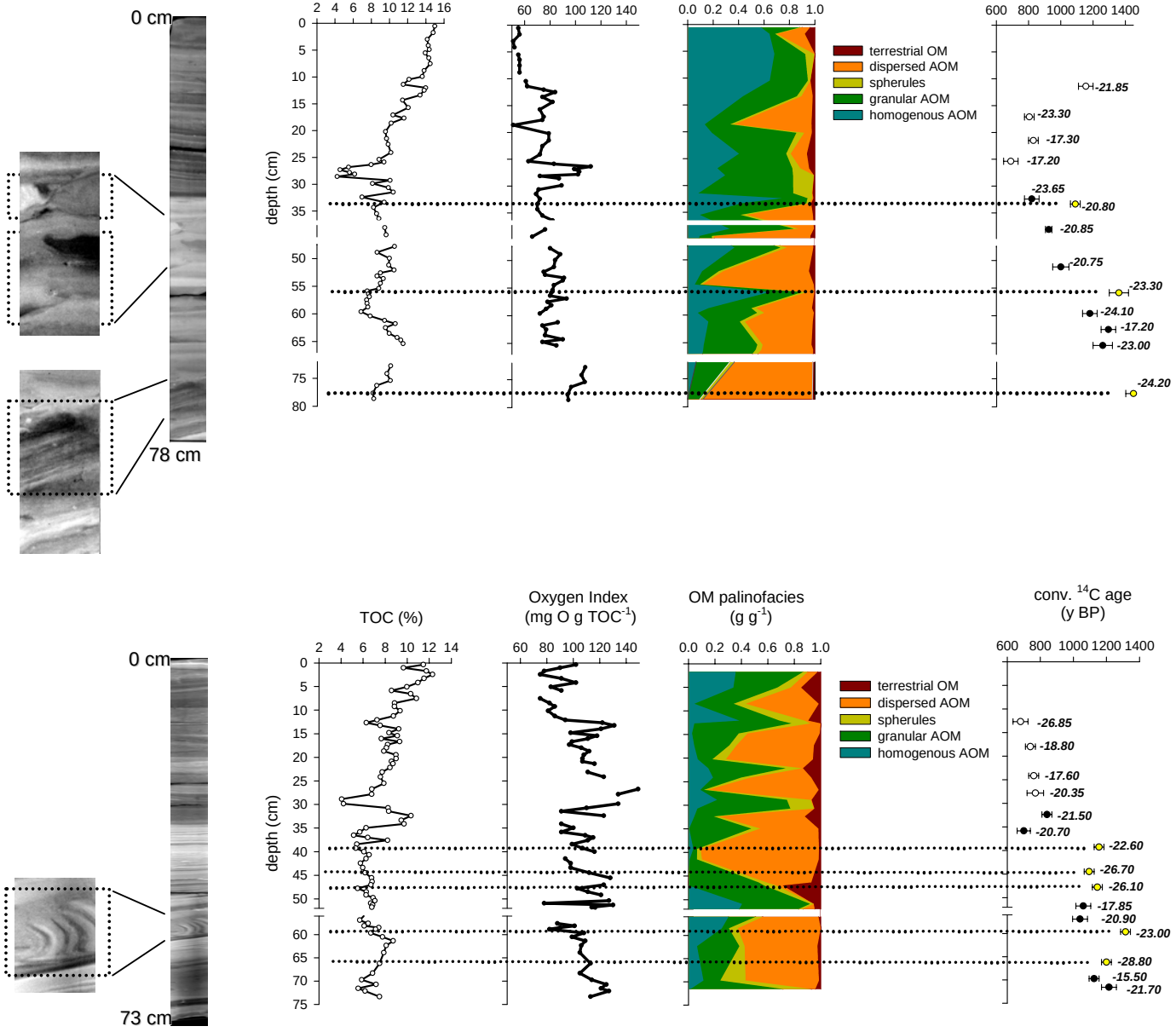
0 cm
78 cm
TOC (%)
Oxygen Index (mg O g TOC-1)
OM palinofacies (g g-1)
conv. 14C age (y BP)
depth (cm)
terrestrial OM
dispersed AOM
spherules
granular AOM
homogenous AOM
-21.85
-23.30
-17.30
-17.20
-23.65
-20.80
-20.85
-20.75
-23.30
-24.10
-17.20
-23.00
-24.20
a
0 cm
73 cm
TOC (%)
Oxygen Index (mg O g TOC-1)
OM palinofacies (g g-1)
conv. 14C age (y BP)
depth (cm)
terrestrial OM
dispersed AOM
spherules
granular AOM
homogenous AOM
-26.85
-18.80
-17.60
-20.35
-21.50
-20.70
-22.60
-26.70
-26.10
-17.85
-20.90
-23.00
-28.80
-15.50
-21.70
b

SF3

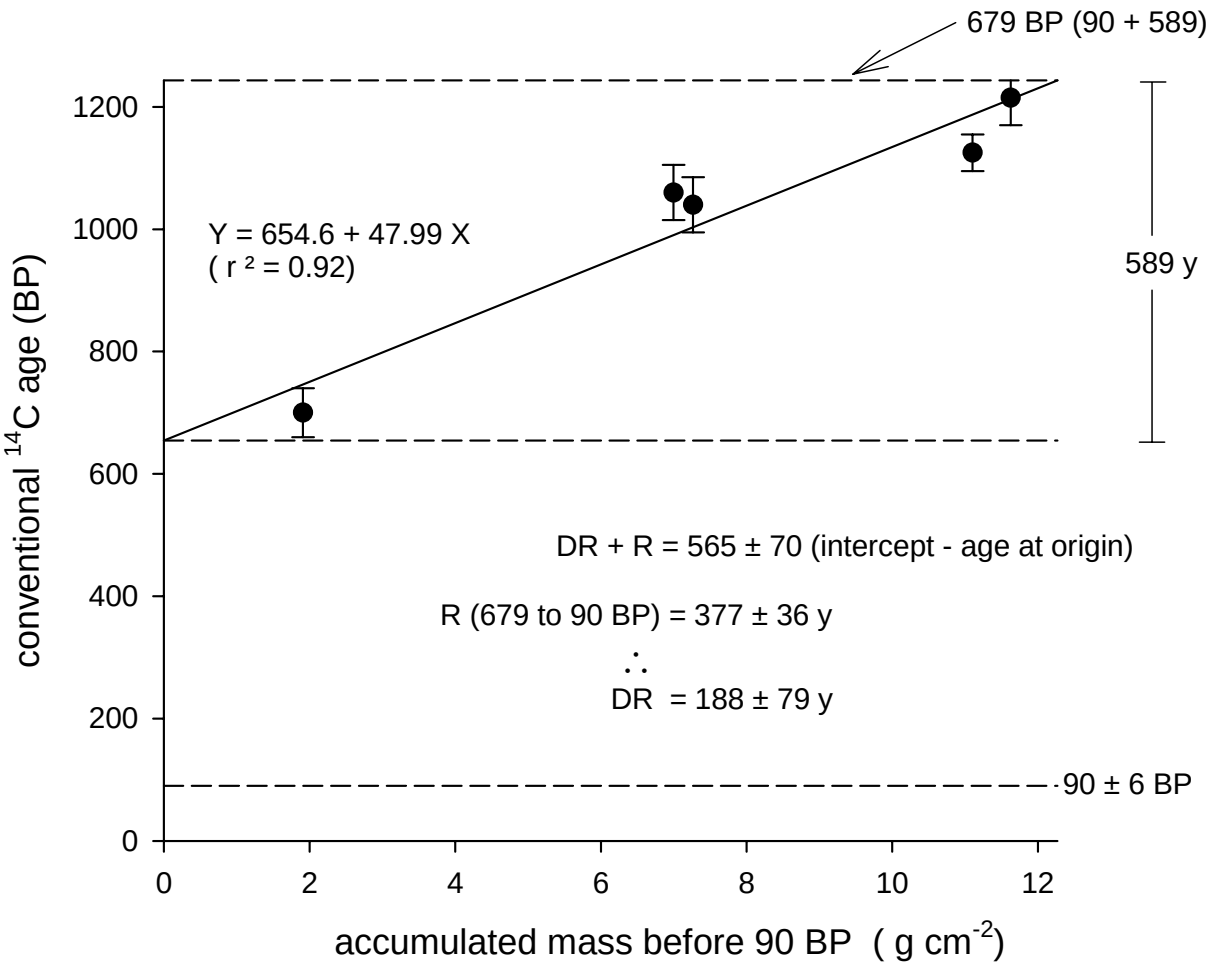
679 BP (90 + 589)
Y = 654.6 + 47.99 X
(r ² = 0.92)
589 y
DR + R = 565 ± 70 (intercept - age at origin)
R (679 to 90 BP) = 377 ± 36 y
∴
DR = 188 ± 79 y
90 ± 6 BP
conventional ^{14}C age (BP)
accumulated mass before 90 BP (g cm^{-2})
0
200
400
600
800
1000
1200
0
2
4
6
8
10
12